

# Biocomposites Scaffolds for Bone Tissue Engineering

I. Olivas-Armendáriz<sup>1</sup>, E. Santos-Rodríguez<sup>2</sup>, M. L. Alvarado-Gutiérrez<sup>3</sup>, Z. A. Meléndez-Molina<sup>3</sup>,  
L. A. Márquez-Chávez<sup>1</sup>, L. E. Valencia-Gómez<sup>1</sup>, C. L. Vargas-Requena<sup>3</sup>, S. A. Martel-Estrada<sup>4,\*</sup>

<sup>1</sup>Instituto de Ingeniería y Tecnología, Universidad Autónoma de Ciudad Juárez, UACJ, Ave. del Charro 450 Norte, Cd. Juárez, Chih. México  
<sup>2</sup>MCTP/UNACH, Ciudad Universitaria Carretera Emiliano Zapata Km. 4, Real del Bosque (Terán). Tuxtla Gutiérrez, Chiapas, México  
<sup>3</sup>Instituto de Ciencias Biomédicas, Universidad Autónoma de Ciudad Juárez, Henry Dunant 4016, Zona Pronaf, Cd. Juárez, Chihuahua, México  
<sup>4</sup>Instituto de Arquitectura, Diseño y Arte, Universidad Autónoma de Ciudad Juárez, UACJ, Ave. del Charro 450 Norte, Cd. Juárez, Chih. México

**Abstract** Chitosan/Extract of *Mimosa tenuiflora* composite scaffolds were fabricated by freeze-drying lyophilization and were then evaluated and compared for use as a bone regeneration scaffold through the evaluation of its bioactivity and biocompatibility. The *in vitro* bioactivity evaluation of the scaffolds was carried out by analyzing the apatite layers produced on them using simulated body fluid (SBF) as an incubation medium. The apatite formation was analyzed using FTIR spectroscopy and Field Emission Scanning Electron Microscopy coupled with energy-dispersive electron X-ray spectroscopy. The cumulative results obtained from IR spectra and SEM-EDS suggest that the developed composites might have potential applications in tissue engineering. The *in vitro* cell culture of Wistar rat's osteoblasts were used to evaluate the phenotype expression of cells in the scaffolds, characterizing the cellular adhesion, proliferation, and alkaline phosphatase activity. Our results, thus, show that Ch/Extracts of *M. tenuiflora* scaffolds are suitable for biological applications.

**Keywords** Chitosan, Mimosa Tenuiflora, Biocompatibility, Bioactivity

## 1. Introduction

The scaffold material that mimics the structure and mechanical properties of the natural bone is an interesting topic in bone tissue engineering. These scaffolds should have a highly porous matrix for the transportation of nutrients, oxygen and metabolic products [1]. In addition, the chemical composition and surface chemistry play an important role in promoting proliferation and differentiation of cells, including the apatite-forming bioactivity for potential use in bone [2]. The mineralization of materials is carried out in a solution containing ions with type and concentrations similar to those existing in the human body, that are called simulated body fluid (SBF) [3].

Polymeric scaffolds and their composites are commonly used in tissue engineering. Polymer-based composites with bioactive ceramic particles were used to improve osteoconductivity and bioactivity [4]. On the other hand, natural products are considered as a source of molecules for the effective treatment of diseases [5]. The medicinal importance of plants is due to the presence of flavonoids, alkaloids, terpenoids, tannins, steroids [6], polyphenols, and

polysaccharides that act specifically on the relevant cells [7].

Chitosan (Ch) is a natural biopolymer in the biomedical area due to their excellent biological properties, such as biocompatibility, biodegradability, and nontoxic properties [8]. Functional groups, such as carboxyl and hydroxyl groups, facilitate the entrapment of biological particles such as antibiotics, growth factors, proteins, and bone forming cells [9].

*Mimosa tenuiflora* (*M. tenuiflora*) (Willd.) Poiré is a plant native of Northeast Brazil and Southeast Mexico and is popularly known as “jurema-preta” and “tepezcohuite,” respectively [10]. The plant is rich in tannins [11], alkaloids, lipids, lupeol, kukulkanins, saponins, and arabinogalactans [12]. The powdered bark has been traditionally used to treat skin burns and wounds and prevent inflammation [12]. Previous studies performed with *M. tenuiflora* confirmed that fibroblast reacts with a strong improvement of viability and proliferation in the presence of arabinogalactan polymers from the plant [12] and also can stimulate monocytes to release TNF- $\alpha$  [13].

Arabinogalactans-proteins (AGPs) are glycosylated proteins of the hydroxyl-rich glycoprotein family. It has been reported that these proteins contain 90–99% of carbohydrate and 1–10% of amino acid. The carbohydrate moiety of AGPs is rich in galactose and arabinose. The AGPs are a water soluble polysaccharide [14] that are highly biocompatible [15].

\* Corresponding author:

mizul@yahoo.com (S. A. Martel-Estrada)

Published online at <http://journal.sapub.org/cmaterials>

Copyright © 2015 Scientific & Academic Publishing. All Rights Reserved

With these characteristics, it could be reasonable to believe in the bioactivity and biocompatibility of a Chitosan/Extract of *M. tenuiflora*. Therefore, in this study, different biodegradable and biocompatible Chitosan/Extract of *M. Tenuiflora* composites were manufactured through thermally induced phase separation method. These composites were used to investigate the *in vitro* biodegradation and *in vitro* bioactivity of scaffolds by analyzing the apatite layers produced in them using SBF as an incubation medium. The apatite formation was analyzed using Fourier Transform Infrared spectroscopy, X-ray Diffraction, Field Emission Scanning Electron Microscopy (SEM), and Energy Dispersive Spectrometry. Moreover, *in vitro* cell culture of Wistar rat osteoblasts was used to evaluate the phenotype expression of cells in the scaffolds, characterizing the cellular adhesion, proliferation and alkaline phosphatase activity.

## 2. Materials and Methods

### 2.1. Materials

Chitosan was purchased from Sigma (United States). The bark of *M. tenuiflora* was obtained from the region of Jiquipilas, Chiapas. Glacial acetic acid (Mallinckrodt, United States) was used as the solvent. SBF was prepared in our laboratory as a previously published method [16].

### 2.2. Characterization of Metabolites from Extract of *Mimosa Tenuiflora*

An amount of 0.5 ml of the *M. tenuiflora* extract of was collected and tested with the addition of a few drops of Mayer's reagent to obtain the cream color precipitation for confirming the presence of alkaloids [17]. To evaluate the presence of steroids and triterpenoids, the Liebermann - Burchard reaction was used [6]. In addition, the extract was also examined for the presence of saponins using 4 ml of the extract and shaking for 2 minutes until it formed foam, which was stable for 15 min or more. Then 1% FeCl<sub>2</sub> was used in water for phenols detection and gelatin-salt test for tannins [18]. For the flavonoid test, 4 ml of the extract was used, and 3 ml of ethanol was added to it. Then magnesium powder and a few drops of concentrated HCl were added [18]. For the quinones test, 1 ml of H<sub>2</sub>SO<sub>4</sub> was added to 3 ml of the extract. The mixture was heated to evaporation point to produce the hydrolysis. Then 5 ml of toluene was added. About 2 ml of this organic phase was taken and then 1 ml of 5% NaOH in 2% ammonia was added to it [19].

The presence of an AGP was confirmed using a qualitative test by Yariv reagent (  $\alpha$ -D-Glucosyl Yariv Reagent, Biosupplies). A radial agar diffusion test [13] was slightly modified and used to measure the AGP content in the arabinogalactans solution. Briefly, agarose gel (1%) containing 0.15 M of sodium chloride, 0.02% sodium azide and 0.002% of Yariv reagent was poured into an 80 mm Petri dish. The gel was allowed to dry at room temperature, and

then wells were punched. A solution gum Arabic (0.01 g/ml) and distilled water were used as a positive and negative control, respectively. Petri dishes were incubated in the dark at room temperature for 2–4 days until a precipitin halo developed.

### 2.3. Preparation of Composites

Ethanol precipitated extract of *M. tenuiflora* was obtained by a method similar to the one proposed by Zippel [12]. Briefly, 50 g of powdered bark from *M. tenuiflora* was mixed with 200 mL of distilled water and mixed for 3 days under strong stirring. After every 20 h, the solution was filtered by gravity three times. Then the extract was filtered, concentrated in a vacuum oven at 37°C. Then the solution was resuspended in 200 mL of water, and the extract was precipitated into 800 mL of ice-cold ethanol (96%). The resultant precipitate was isolated by centrifugation for 10 min (3000 rpm), dissolved in 15 mL of water, and dialyzed with cellulose membranes (MWCO 3.5 kDa). The resultant of the dialyzed procedure was yield to 15 mL with distilled water. This solution is the arabinogalactans solution, which was used for the composite preparation.

Chitosan/extract of *M. tenuiflora* composites were prepared in our laboratory according to the procedure described below. Our goal was to prepare compositions that contain exactly the quantity of metabolites contained in 80/20 and 70/30 composites of Chitosan/Bark of *M. tenuiflora* in weight. Two types of composites were prepared. The 80/20 composite corresponded to 0.300 mL of ethanol extract solution by each 4 g of chitosan. The 70/30 composite corresponded to 0.450 mL of ethanol extract solution by each 3.5 g of chitosan. The ethanol extract solution and chitosan were dissolved in 1% (%v/v) aqueous acetic acid solution. Finally, the composites were frozen and freeze-dried for 2 days.

### 2.4. Characterization of Morphology and *in vitro* Bioactivity

For the *in vitro* bioactivity study, porous samples of approximately 1 cm  $\times$  0.5 cm  $\times$  0.5 cm were soaked in 5 mL of tetraethoxyl orthosilicate for 2 h in a vacuum oven at 60 °C. Then the samples were rinsed with ethanol and dried in still air at room temperature for 24 h. Afterward, the samples were soaked in 5 mL of 1.5X SBF, pH 7.4 for different periods of time in an incubator at 37 °C. The solution was refreshed every 48 h. After the incubation period, the samples were rinsed with deionized water and dried.

In order to characterize the morphology, a Field Emission SEM JEOL JSM-7000F coupled with an energy-dispersive system EDS 7557 INCA Oxford Instruments (England) were used. The Ca/P ratio was estimated for the various conditions. The pore size was measured using the Scandium Universal SEM Imaging Platform software. Three different cross-sections of each scaffold were used with at least 120 pores. The porosity was determined by a liquid displacement

method used previously [8].

## 2.5. FTIR and XRD Spectroscopy

The chemical characterization was evaluated in FTIR. FTIR spectra were recorded using a transmission mode in an IR spectrometer (Nicolet 6700, Thermo Scientific, USA). For each spectrum, 100 scans at 16 cm<sup>-1</sup> resolution were averaged.

## 2.6. In vitro Degradation

Chitosan/extract of *M. tenuiflora* scaffolds were immersed in PBS (pH 7.4, containing NaN<sub>3</sub>). Scaffolds of uniform dimensions approximately 1 cm × 0.5 cm × 0.5 cm (3 mm) were used to perform a degradation test. Samples were collected after predetermined time periods (1, 3, 7, 10 and 14 days), washed with DI water, and dried at room temperature for 2 days. The remaining weight of the scaffolds was determined using the following equation (n = 3):

$$\text{Weight loss (\%)} = [(w_i - w_d)/w_i \times 100]$$

Where  $w_i$  is the initial weight of the scaffold and  $w_d$  is the dry weight of the scaffolds after incubation.

## 2.7. Cell Harvesting and Culture

About 2 weeks old Sprague-Dawley rats were used for the isolation of osteoblasts from calvarian. The rat calvaria tissues were dissected and dissociated [20]. The scaffolds were sterilized by exposition to UV light for 2 h and then osteoblasts calvaria cells were pooled into the scaffolds at a density of 50,000 cells/cm<sup>2</sup> and cultured in the prepared solution of  $\alpha$ -MEM supplemented with 10% fetal bovine, 1% antibiotics, 2.1 mg/ml  $\beta$ -glycerophosphate, and 50  $\mu$ g/ml ascorbic acid in an incubator at 37°C with 5% CO<sub>2</sub>. Cultures were finished at 24 and 72 h.

## 2.8. Scanning Electron Microscopy (SEM) Examination of Cell-seeded Scaffolds

After being cultured for different times, the samples with attached cells were rinsed twice with PBS (pH 7.4) and immersed in PBS containing 3% glutaraldehyde for 4 h to fix the cells, followed by rinsing twice with PBS for 10 min and finally dehydrated through a series of graded ethanol solutions. A field emission SEM JEOL JSM-7000F coupled with an energy-dispersive system EDS 7557 INCA Oxford Instruments (England) were used to characterize them.

## 2.9. Biochemical and Differentiation Analyses

Scaffolds with osteoblasts calvaria cells with a density of 50,000 cells/cm<sup>2</sup> were used as a culture test. The cells were cultured in the prepared solution of  $\alpha$ -MEM supplemented with fetal bovine, antibiotics,  $\beta$ -glycerophosphate and ascorbic acid in an incubator at 37°C with 5%. Control and test cultures were harvested at 24 and 72 h and washed twice with PBS. The osteoblasts were lysed with 3 ml of 1% Triton X-100 in DEPC-treated water and three freeze-thaw cycles at -70°C. The alkaline phosphatase activity in the lysed cells

was determined using an alkaline phosphatase substrate assay kit and the absorbance measured at 405 nm.

## 2.10. Cell Viability and Proliferation

The cell viability was determined using a previous method [21]. Briefly, 3-(4,5-dimethylthiazol-2-yl)-2,5-diphenyltetrazolium bromide (MTT) assay was used. At each cultured time, MTT solution (50  $\mu$ L) and  $\alpha$ -MEM (450  $\mu$ L) containing FBS and antibiotic were added to each composite. After 3 h of incubation, 400  $\mu$ L of dimethyl sulfoxide (DMSO) was added to dissolve the formazan product, and the absorbance was measured at 570 nm. The cell number was determined with a standard curve. The analysis of cell was evaluated using a Quant-iT™ PicoGreen dsDNA kit. The fluorescence emission intensity was measured at 520 nm. The amount of DNA was determined based on the standard curve.

## 2.11. Statistical Analysis

The data obtained were evaluated for statistical significance using the Student's t-test. The results are reported as mean  $\pm$  standard deviation (SD), and the differences observed between composites results were considered significant when  $p < 0.05$ .

# 3. Results and Discussion

## 3.1. Characterization of Metabolites from Extract of *Mimosa Tenuiflora*

*M. tenuiflora* has been used for wound healing and treatment of skin burns in Central and South America [12]. The high content of saponin and tannins is considered the cause of its healing properties due to antimicrobial, anti-inflammatory and cicatrizing effects [12, 22]. The dried bark of *M. tenuiflora* is highly rich in steroidal saponins [23]. The procedure used in this research to get the extract of *M. tenuiflora* was the one proposed previously by other researchers [12]. They found that the extract was composed mainly by arabinose, galactose (arabinogalactans), glucose, mannose and galacturonic acid. We also detected the presence of alkaloids, saponins, flavonoids, quinones and arabinogalactans (Figure 1). For this research, it was very important to find evidence of flavonoids because these metabolites possess a therapeutic potential in some human disorders. They exhibit an antioxidant activity inactivating free radical or preventing decomposition of hydroperoxides into free radicals. In addition, flavonoids exhibit antioxidative, antiviral, antimicrobial, antiplatelet and antitoxic activities [24]. Moreover, bioflavonoids have been associated with bone health and osteoblast differentiation *in vitro* [25]. On the other hand, the biological roles of alkaloids include both anti-inflammatory and antibacterial effects [26, 27]. Furthermore, some chromone alkaloids have been associated with osteoclast differentiation inhibitory activity that could promote a better bone regeneration in patients

with osteoporosis [28]. Finally, the extract of *M. tenuiflora* had evidence of arabinogalactans. It had been found that arabinogalactans are potent stimulators of dehydrogenase activity and proliferation of skin fibroblasts, with a strong improvement in viability and proliferation [12]. Although it has been reported that the cortex contains phenols, tannins, steroids and triterpenoids [12, 29], we did not find any evidence of these secondary metabolites from the ethanol fraction obtained in our research.

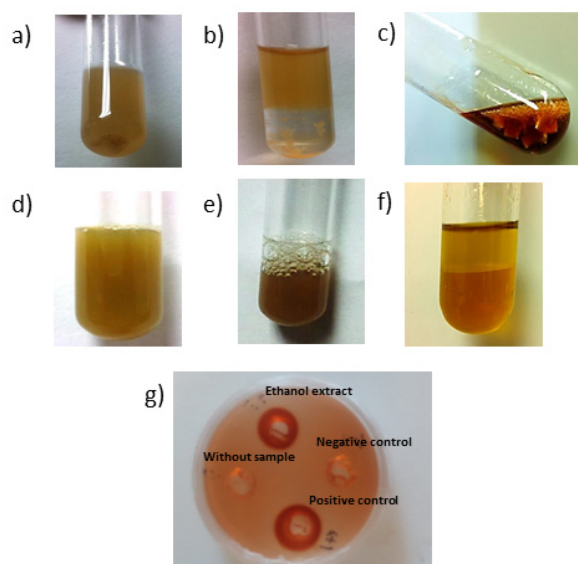


**Figure 1.** Identification of metabolites in the extract of *M. tenuiflora*, a) alkaloids positive, b) phenols and tannins negative, c) flavonoids positive, d) steroids and/or triterpenoid negative, e) Saponins positive, f) quinones positive, and g) arabinogalactans positive

### 3.2. Morphology and in Vitro Bioactivity of the Scaffolds

Chitosan is a material with favorable degradability, antimicrobial activity, thermal stability and biocompatibility [30]. Nevertheless, the use of chitosan in tissue engineering has some limitations, including loss of bioactivity [31, 32]. The bioactivity could be measured when the material shows a kinetic modification in a surface layer during a certain period after the implantation [33]. In essence, it refers to inducing precipitation and mineralization of calcium phosphate on the surface [30]. This modification is a carbonated hydroxyapatite layer, which is chemically and structurally equivalent to a mineral phase in bone and provides an interface link between materials and tissues. In this way, the bioactivity of artificial materials could be attributed to the formation of an active layer of hydroxyapatite [33].

The process of formation of hydroxyapatite in bioactive materials can be reproduced in an SBF, which can predict the *in vivo* bone bioactivity. SBF has been used in different concentrations including from 1x until 5x [32, 34]. Its main advantage is that SBF is a biomimetic method that does not require a special equipment or process of high temperatures to produce a hydroxyapatite layer. The properties of this layer can affect the cell viability and proliferation [32]. The

process of apatite formation requires consumption of calcium and phosphate ions from the surrounding body fluid. The calcium phosphate uses  $\text{OH}^-$ ,  $\text{CO}_3^{2-}$ ,  $\text{Na}^+$ ,  $\text{K}^+$  and  $\text{Mg}^{2+}$  ions from the SBF solution until it crystallizes into hydroxyapatite [35].

Scaffolds are used for bone tissue regeneration in order to provide an environment for the bone formation, including porous structures that are essential for cell migration, bone tissue ingrowth, vascularization and exchange of nutrients and waste [36, 37]. During this study, the composites obtained consisted of pores mainly in deep planes of the scaffold and few pores at the surface. Pores with sizes around 100  $\mu\text{m}$  play an important role in bone ingrowth [8]. It has been estimated that optimal pore size varies from 150 to 500  $\mu\text{m}$  [38]. The 80/20 composite (Figure 2) showed porosity around 100  $\mu\text{m}$  and 500  $\mu\text{m}$  and small pores between 20 and 80  $\mu\text{m}$  (Table 1).

**Table 1.** Pore size distribution

Composite	0-5 ( $\mu\text{m}$ )	5-10 ( $\mu\text{m}$ )	10-50 ( $\mu\text{m}$ )	50-100 ( $\mu\text{m}$ )	>100 ( $\mu\text{m}$ )
Ch	1.02 %	2.78 %	4.33 %	27.56 %	64.31 %
80/20	0.00 %	1.32 %	1.56 %	3.66 %	93.46 %
70/30	2.13 %	2.59 %	9.54 %	11.42 %	74.32 %

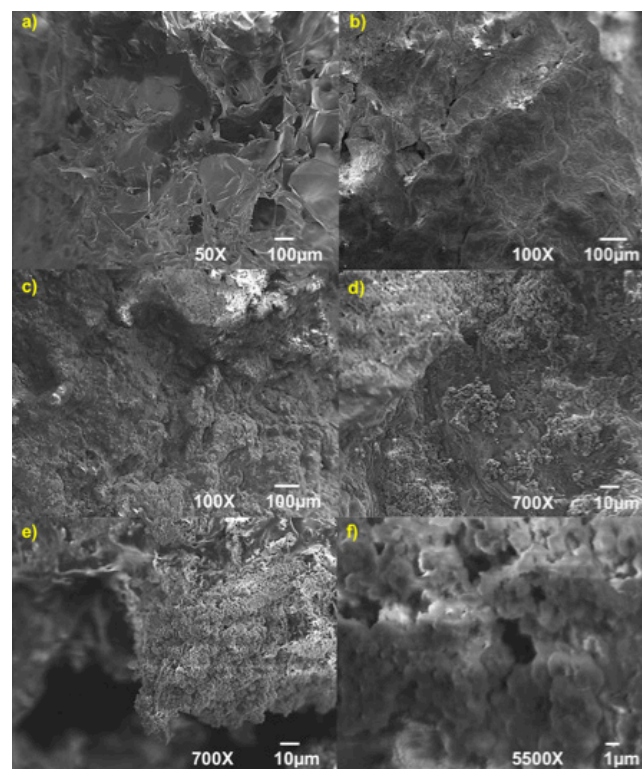


**Figure 2.** Micrographs of a) 80/20 chitosan/extract of *M. tenuiflora* and 80/20 chitosan/extract of *M. tenuiflora* incubated by (b) 21 days, (c) (d) and (e) 28 days at 100X and (f) 28 days at 5500X

After the incubation, many micro particles were observed on the surface of scaffold [3] that agglomerate as they grow to form a continuous uniform layer in a cauliflower-like form composed by spheres of approximately 1–3  $\mu\text{m}$  size. Most of

the globular apatite aggregates have grown either inside the polymeric matrix or on the pore walls [37]. In addition, it can be seen that more layers are superposed to the original aggregates that incorporate the first coating, suggesting the existence of secondary nucleation sites for additional apatite formation, with interconnected successive layers. On the other hand, the 70/30 composite (Figure 3) showed porosity around 150–250  $\mu\text{m}$  and small pores (40–60  $\mu\text{m}$ ). After 21 days of incubation, some pores were degraded and collapsed, and other revealed the formation of apatite crystals in conglomerates with sizes around 10 to 30  $\mu\text{m}$ .

### 3.3. FTIR and XRD of the Samples

Before the SBF treatment, the composites were immersed in tetraethoxysilane (TEOS) to functionalize with the Si-OH groups. These groups act as a nucleation site to accelerate the formation of apatite crystals during the incubation in SBF [37]. During this research, SBF was used to promote that silanol groups attract calcium ions and the deposition of anions in SBF such as phosphate and carbonate [39]. The formation of apatite layer can be reproduced with a cellular SBF with ion concentrations nearly equal to the human blood plasma [31, 40, 41]. Thus, the chemical structure of the incubated composites was analyzed using FTIR. The chemical interaction could be appreciated by analyzing the changes in the characteristic peaks of the substance or the appearance of new peaks [42]. Regarding the hydroxyapatite layers in the FTIR analysis and in order to get a better definition of the hydroxyapatite bands, the original spectra of each composite were subtracted from the one obtained for each SBF treated composite (Figures 4 and 5). The IR analysis for the 80/20 composite revealed the presence of the  $\nu_3$  stretching mode of P-O bonds around 1063  $\text{cm}^{-1}$  and 607  $\text{cm}^{-1}$ , which is evident at 28 days in all composites. The band

at 1409  $\text{cm}^{-1}$  provides evidence of carbonate ( $\text{CO}_3^{2-}$ ) incorporated in the apatite [35]. On the other hand, 70/30 composite revealed bands at 1076  $\text{cm}^{-1}$  corresponding to P-O bonds and bands at 847  $\text{cm}^{-1}$  and 1417  $\text{cm}^{-1}$  for  $\text{CO}_3^{2-}$  bonds. The bands were more evident at 28 days. Therefore, it is possible to suggest that carbonated apatite was formed.

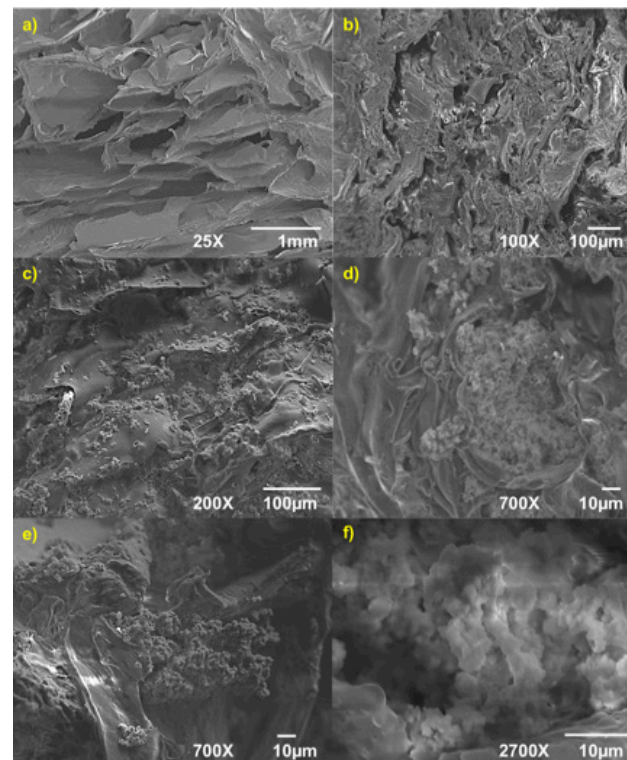


**Figure 3.** Micrographs of a) 80/20 chitosan/extract of *M. tenuiflora*, and 80/20 chitosan/extract of *M. tenuiflora* incubated by (b) 21 days, (c) (d) and (e) 28 days at 100X and (f) 28 days at 5500X

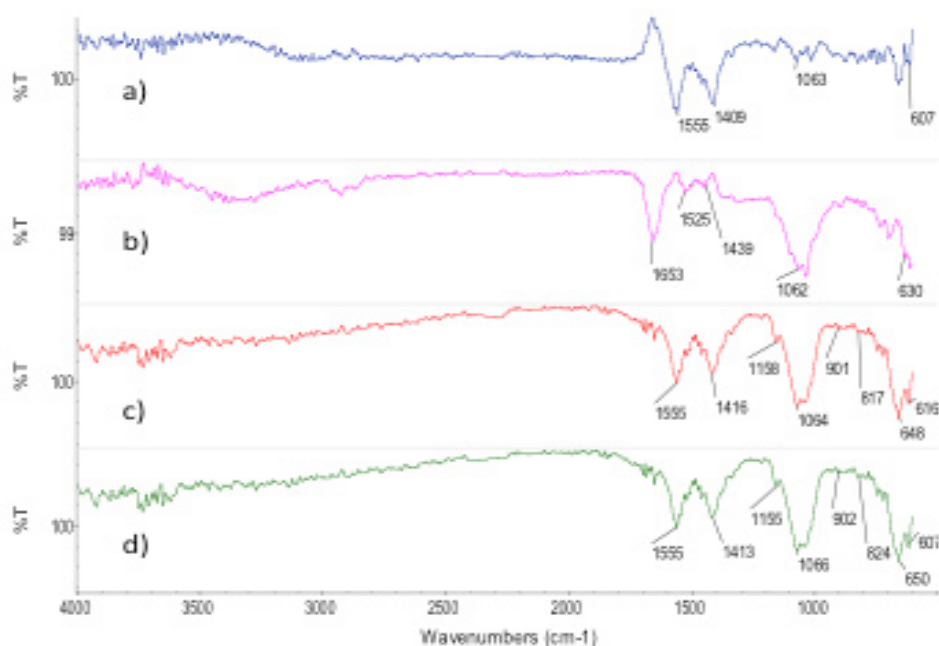


**Figure 4.** FTIR of 80/20 chitosan/extract of from *M. tenuiflora* incubated in 1.5X SBF by (a) 7 days, (b) 14 days, (c) 21 days and (d) 28 days



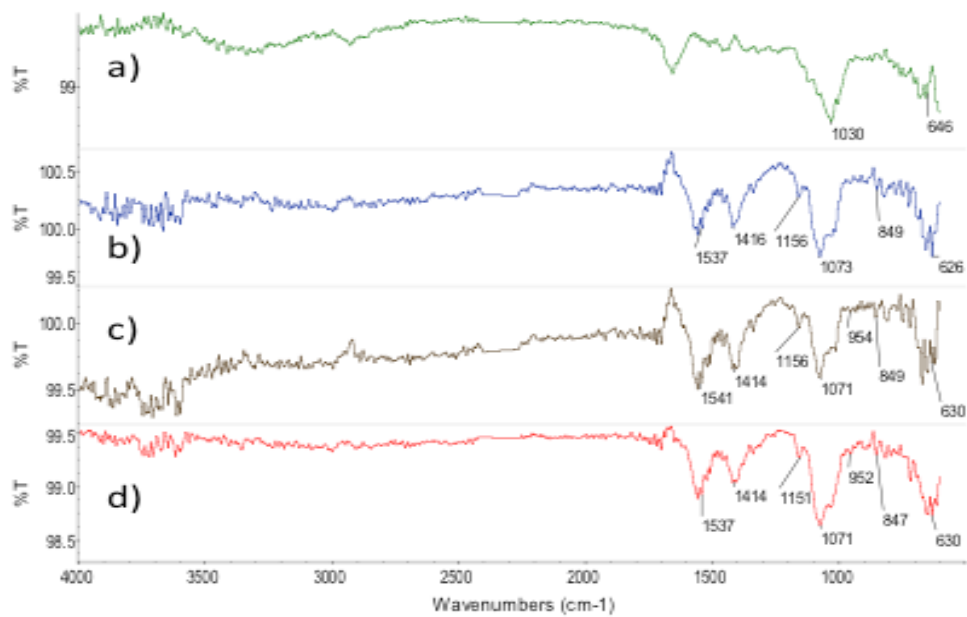


**Figure 5.** FTIR of 70/30 chitosan/extract of *M. tenuiflora* incubated in 1.5X SBF by (a) 7 days, (b) 14 days, (c) 21 days and (d) 28 days

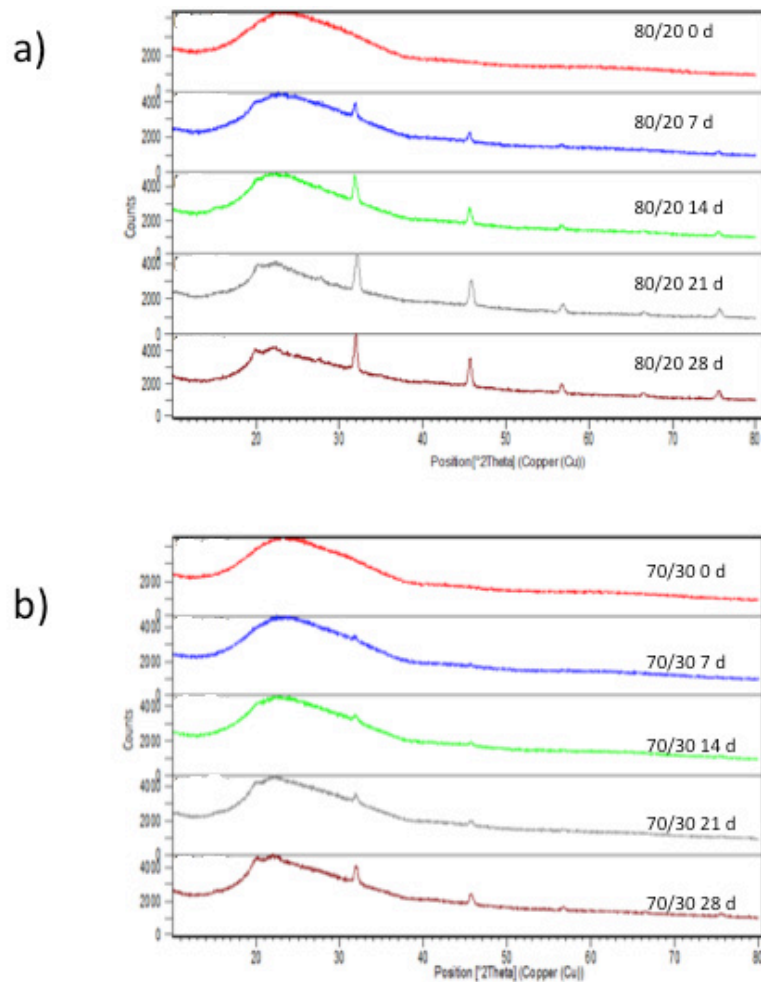


**Figure 6.** XRD diffractograms of a) 80/20 and b) 70/30 chitosan/extract of *Mimosa Tenuiflora* composites before incubation and at 7, 14, 21 and 28 days after incubation in SBF 1.5X at 37° C

XRD patterns (Figure 6) indicate that the strength and width of HA gradually increased with the immersion time, increasing from 1 to 28 days. The XRD diffractograms of composites show a peak of high intensity at  $2\theta=21.70^\circ$  (Figure 8). This peak corresponds to the regular crystal lattice (1 1 0) of chitosan [43]. On the other hand, X-ray diffraction analysis confirmed the peaks of the chitosan/*M. tenuiflora* composite after incubation were sharper and stronger, which suggested that higher levels of crystallinity were formed on the scaffold apatite. The time for formation of apatite crystals on the surface is shown in the X-ray diffraction spectra on Figure 5. For the composites, a peak appearing at  $2\theta=32^\circ$  after immersion became less broad with respect to longer immersion times, suggesting the formation of apatite with higher crystallinity, as reported previously [19]. In addition, it is possible to identify peaks for amorphous calcium at  $2\theta=45^\circ$  and  $2\theta=66.44^\circ$  for  $\text{CaCO}_3$ . It is possible to identify a peak at  $56^\circ$  that corresponds to octacalcium phosphate [44]. Once apatite nuclei are formed, they can grow by consuming calcium and phosphate ions from the SBF solution. The Si-O<sup>-</sup> on the composite attracts a positive Ca layer, which then combines with negatively charged  $\text{PO}_4^{3-}$  [37]. The relative intensities of apatite deposited on the surface of scaffold increased with an immersion time of the composite. Combined with the results of SEM/EDS and FTIR, it can be deduced that the induced apatite was a carbonated HA.

### 3.4. In Vitro Degradation

The degradation rate of scaffold for bone tissue engineering is considered a key factor. The degradation rate must match the ingrowth rate of newly formed bone [45]. *In vitro* degradation of Chitosan/Extract of *M. tenuiflora* composites were assessed by incubating them under physiological conditions and comparing the weight difference before and after each test. As shown in Figure 7, the weight of composites had the tendency to slowly decrease with incubation time. Primary amines capture protons from water and alkalize the culture medium. The pH of the medium was increased because of groups and alkaline ions, which are produced during the degradation of chitosan [46] and *M. tenuiflora*. The amino groups or hydroxyl groups of chitosan can neutralize the effects of the carboxyl groups of *M. tenuiflora* [16].

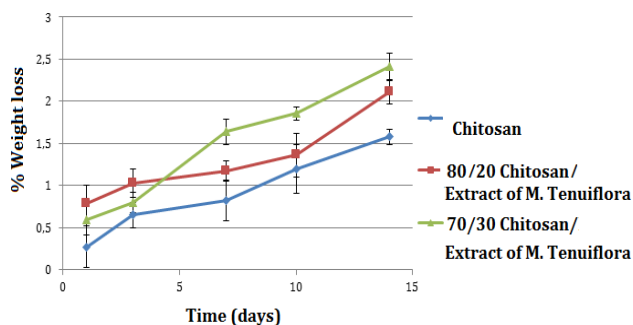


Figure 7. Weight loss of composites of the composites

### 3.5. Cell Viability and Proliferation

The cell culture *in vitro* was used to assess the influence of *M. tenuiflora* of the scaffolds on cell behavior. A bar graph for behavior of the cell number of osteoblasts seeded on different scaffolds is shown in Figure 8. At 72 h, the composite 80/20 Ch/Extract of *M. tenuiflora* shows a significant higher number of cells than the control and chitosan scaffold. After 72 h, the number of cells in 80/20 and 70/30 composites was similar within the same level of significance. These results suggest that the combination between Chitosan and *M. tenuiflora* allows increased viability in different combinations.

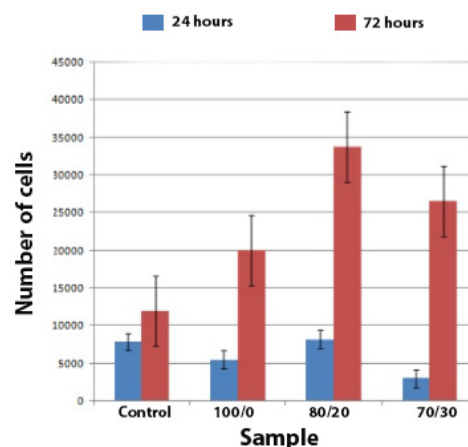


Figure 8. Number of cells after culture 24 h and 72 h

### 3.6. Biochemical and Differentiation Analyses

During the stages in osteoblast differentiation, specific bone proteins are used to monitor osteoblastic phenotype [47]. The primary culture of osteoblasts can express specific proteins, such as ALP, osteocalcin and type I collagen, in the same temporal order like *in vivo* expression [48]. ALP activity is observed at early stages of osteoblast differentiation, particularly during the immature stage [47]. ALP has been associated with the mineralization process, so an increased level of the ALP is a sign of the metabolic activity of the osteoblasts [48].

The bar graph in Figure 9a illustrates the results of the ALP activity of the cells in the scaffolds. All composites showed ALP expression, indicating that the osteoblasts were able to begin the differentiation process. The ALP expression was significantly more in 80/20 composite than in other scaffolds. On the other hand, Figure 9b shows the DNA quantitation of the samples. DNA content results showed different cell proliferation behaviors on the different scaffolds. We noted no significant difference in the cell proliferation at 24 h among the scaffolds. More importantly, significant higher cell numbers were found on the 80/20 scaffolds at 72 h. Considering the number of the cells on all the scaffolds at 24 h were almost the same, the higher cell numbers on the 80/20 scaffolds indicated that better cell compatibility was achieved with this composition.

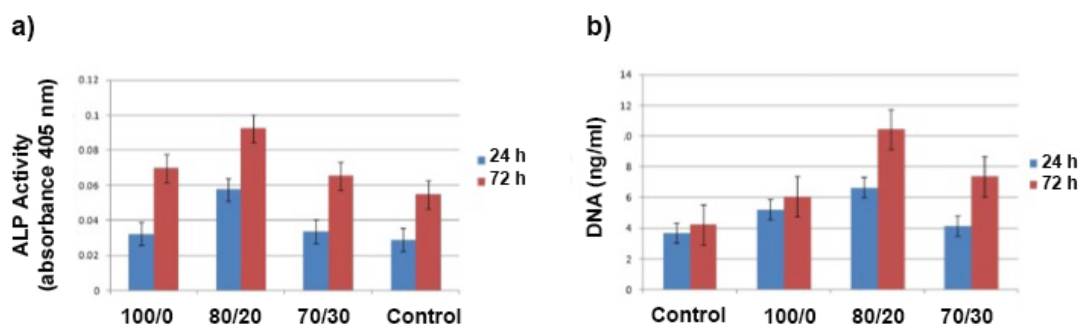


Figure 9. a) ALP activity and DNA quantitation at 24 hours and 72 hours after cell culture

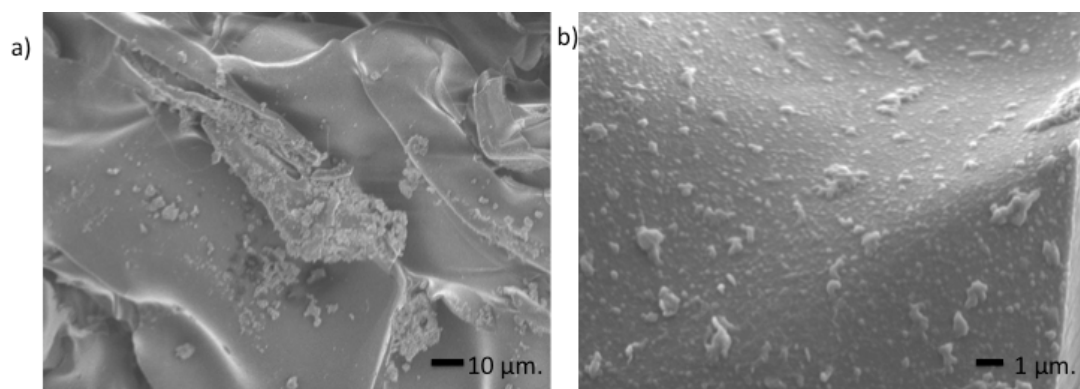


Figure 10. Osteoblasts seeded of the 80/20 chitosan/extract of *M. tenuiflora* scaffolds

Figure 10 shows the presence of a large amount of globular mineral deposits attached to the scaffolds that was also confirmed by SEM micrographs and EDS analysis (Figure 4). This observation showed that a number of cells were well adhered to the scaffold.

Mexican Public Education Secretary and the Mexican National Council for Science and Technology (CONACyT) through project SEP-CONACyT CB 2012-01-180909. Also, we greatly appreciate the support of B.S. Georgina Lopez during the management of the project.

## 4. Conclusions

Chitosan/Extract of *M. tenuiflora* scaffolds were successfully prepared by thermally-induced phase separation technique. An accelerated process of biomineralization with concentrated SBF was used in the assessment of bioactivity of the composite. The chitosan/Extract of *M. tenuiflora* extract composites showed better biomineral activity than chitosan scaffolds. In the scaffolds, polysaccharides from *M. tenuiflora* provided nuclei in the mineralization process. As a result, more apatite was formed on the composite scaffolds than on the chitosan scaffolds. The ability of the composites to form a mineralized layer on their surface was evident by the cumulative results obtained from IR spectra, SEM and EDS. It was demonstrated that the Chitosan/extract of *M. tenuiflora* composites were able to induce the bone-like apatite nucleation and growth on their surfaces from SBF. In addition, it was demonstrated that the composites promote biocompatibility with osteoblasts cells.

## ACKNOWLEDGEMENTS

The authors acknowledge the financial support of the

## REFERENCES

- [1] Milovac D, Gallego Ferrer G, Ivankovic M, Ivankovic H. PCL-coated hydroxyapatite scaffold derived from cuttlefish bone: morphology, mechanical properties and bioactivity. *Materials science & engineering C, Materials for biological applications* 2014;34:437-45.
- [2] Chen J, Que W, Xing Y, Lei B. Fabrication of biomimetic polysiloxane-bioactive glass-chitosan hybrid monoliths with high apatite-forming bioactivity. *Ceramics International* 2015;41, Supplement 1:S393-S8.
- [3] El-Maghraby HF, Gedeon O, Rohanova D, Greish YE. Compressive strength and preliminary in vitro evaluation of gypsum and gypsum-polymer composites in protein-free SBF at 37°C. *Ceramics International* 2010;36:1561-9.
- [4] Tamjid E, Bagheri R, Vossoughi M, Simchi A. Effect of particle size on the in vitro bioactivity, hydrophilicity and mechanical properties of bioactive glass-reinforced polycaprolactone composites. *Materials Science and Engineering: C* 2011;31:1526-33.
- [5] Osadebe PO, Omeje EO. Comparative acute toxicities and immunomodulatory potentials of five Eastern Nigeria mistletoes. *Journal of ethnopharmacology* 2009;126:287-93.



- [6] Samejo MQ, Memon S, Bhanger MI, Khan KM. Isolation and characterization of steroids from *Calligonum polygonoides*. *Journal of Pharmacy Research* 2013; 6:346-9.
- [7] Giacomini F, Pier, G., Souza, E., Lechtenberg, M., Petereit, F., Palazzo, J., Hensel, A. Hydrolyzable tannins from hydroalcoholic extract from *Poincianella pluviosa* stem bark and its wound-healing properties: Phytochemical investigations and influence on in vitro cell physiology of human keratinocytes and dermal fibroblasts. *Fitoterapia* 2014; 99: 252-60.
- [8] Wang D, Zhang Y, Hong Z. Novel fast-setting chitosan/ $\beta$ -dicalcium silicate bone cements with high compressive strength and bioactivity. *Ceramics International* 2014; 40:9799-808.
- [9] Chen Q, Cabanas-Polo S, Goudouri OM, Boccaccini AR. Electrophoretic co-deposition of polyvinyl alcohol (PVA) reinforced alginate-Bioglass(R) composite coating on stainless steel: Mechanical properties and in-vitro bioactivity assessment. *Materials science & engineering C, Materials for biological applications* 2014;40:55-64.
- [10] Silva VA, Gonçalves GF, Pereira MSV, Gomes IF, Freitas AFR, Diniz MFFM, et al. Assessment of mutagenic, antimutagenic and genotoxicity effects of *Mimosa tenuiflora*. *Revista Brasileira de Farmacognosia* 2013; 23:329-34.
- [11] Oliveira LM, Macedo IT, Vieira LS, Camurca-Vasconcelos AL, Tome AR, Sampaio RA, et al. Effects of *Mimosa tenuiflora* on larval establishment of *Haemonchus contortus* in sheep. *Veterinary parasitology* 2013;196:341-6.
- [12] Zippel J, Deters A, Hensel A. Arabinogalactans from *Mimosa tenuiflora* (Willd.) Poir bark as active principles for wound-healing properties: specific enhancement of dermal fibroblast activity and minor influence on HaCaT keratinocytes. *Journal of ethnopharmacology* 2009;124: 391-6.
- [13] Gannabathula S, Krissansen GW, Skinner M, Steinhorn G, Schlothauer R. Honeybee apisimin and plant arabinogalactans in honey costimulate monocytes. *Food chemistry* 2015; 168:34-40.
- [14] Goellner EM, Utermohlen J, Kramer R, Classen B. Structure of arabinogalactan from *Larix laricina* and its reactivity with antibodies directed against type-II-arabinogalactans. *Carbohydrate Polymers* 2011;86:1739-44.
- [15] Boudjeko T, Rihouey C, Ndoumou DO, El Hadrami I, Lerouge P, Driouch A. Characterisation of cell wall polysaccharides, arabinogalactans-proteins (AGPs) and phenolics of *Cola nitida*, *Cola acuminata* and *Garcinia kola* seeds. *Carbohydrate Polymers* 2009;78:820-7.
- [16] Martel-Estrada SA, Olivas-Armendáriz I, Santos-Rodríguez E, Martínez-Pérez CA, García-Casillas PE, Hernández-Paz J, et al. Evaluation of in vitro bioactivity of Chitosan/*Mimosa tenuiflora* composites. *Materials Letters* 2014;119:146-9.
- [17] Kamala K, Sivaperumal P, Gobalakrishnan R, Swarnakumar NS, Rajaram R. Isolation and characterization of biologically active alkaloids from marine actinobacteria *Nocardopsis* sp. NCS1. *Biocatalysis and Agricultural Biotechnology* 2015;4: 63-9.
- [18] Jones W, Kinghorn, D. Extraction of plant secondary metabolites. In: Sarker S, Latif, Z., Gray I., editor. *Natural product isolation*. Totowa, NJ: Humana Press Inc; 2006.
- [19] Jain P, Jain, S., Pareek, A., Sharma, S. A comprehensive study on the natural plant phenols: perception to current scenario. *Bulletin of Pharmaceutical Research* 2013;3: 90-106.
- [20] Martel-Estrada SA, Olivas-Armendariz I, Martinez-Perez CA, Hernandez T, Acosta-Gomez EI, Chacon-Nava JG, et al. Chitosan/poly(DL,lactide-co-glycolide) scaffolds for tissue engineering. *Journal of materials science Materials in medicine* 2012; 23:2893-901.
- [21] Martel-Estrada SA, Rodríguez-Espinoza B, Santos-Rodríguez E, Jiménez-Vega F, García-Casillas PE, Martínez-Pérez CA, et al. Biocompatibility of chitosan / *Mimosa tenuiflora* scaffolds for tissue engineering. *Journal of Alloys and Compounds* 2015.
- [22] Moncao NB, Araujo BQ, Silva Jdo N, Lima DJ, Ferreira PM, Airoidi FP, et al. Assessing chemical constituents of *Mimosa caesalpinifolia* stem bark: possible bioactive components accountable for the cytotoxic effect of *M. caesalpinifolia* on human tumour cell lines. *Molecules* 2015;20:4204-24.
- [23] Rivera-Arce E, Gattuso M, Alvarado R, Zarate E, Aguero J, Feria I, et al. Pharmacognostical studies of the plant drug *Mimosa tenuiflora* cortex. *Journal of ethnopharmacology* 2007;113:400-8.
- [24] Soumaya K-J, Zied G, Nouha N, Mounira K, Kamel G, Genviève FDM, et al. Evaluation of in vitro antioxidant and apoptotic activities of *Cyperus rotundus*. *Asian Pacific Journal of Tropical Medicine* 2014;7:105-12.
- [25] Lee MK, Lim SW, Yang H, Sung SH, Lee H-S, Park MJ, et al. Osteoblast differentiation stimulating activity of biflavonoids from *Cephalotaxus koreana*. *Bioorganic & Medicinal Chemistry Letters* 2006;16:2850-4.
- [26] Cushnie TPT, Cushnie B, Lamb AJ. Alkaloids: An overview of their antibacterial, antibiotic-enhancing and antivirulence activities. *International Journal of Antimicrobial Agents* 2014; 44:377-86.
- [27] Qiu S, Sun H, Zhang A-H, Xu H-Y, Yan G-L, Han Y, et al. Natural alkaloids: basic aspects, biological roles, and future perspectives. *Chinese Journal of Natural Medicines* 2014; 12:401-6.
- [28] Morita H, Nugroho AE, Nagakura Y, Hirasawa Y, Yoshida H, Kaneda T, et al. Chrotacumines G-J, chromone alkaloids from *Dysoxylum acutangulum* with osteoclast differentiation inhibitory activity. *Bioorganic & Medicinal Chemistry Letters* 2014; 24:2437-9.
- [29] Jiag Y, Haag, M. Structure of a new saponin from the bark of *Mimosa tenuiflora*. *Journal of Natural Products* 1991;54: 1247-53.
- [30] Zhang J, Dai C, Wei J, Wen Z, Zhang S, Chen C. Degradable behavior and bioactivity of micro-arc oxidized AZ91D Mg alloy with calcium phosphate/chitosan composite coating in m-SBF. *Colloids and Surfaces B: Biointerfaces* 2013;111: 179-87.
- [31] I.B. Leonor AI, K. Onuma, N. Kanzaki, R.L. Reis. In vitro bioactivity of starch thermoplastic/hydroxyapatite composite biomaterials: an in situ study using atomic force microscopy. *Biomaterials* 2003;24:579-85.
- [32] Kong L, Gao Y, Lu G, Gong Y, Zhao N, Zhang X. A study on the bioactivity of chitosan/nano-hydroxyapatite composite

- scaffolds for bone tissue engineering. *European Polymer Journal* 2006; 42:3171-9.
- [33] Wopenka B, Pasteris, J. A mineralogical perspective on the apatite in bone. *Materials science & engineering C* 2005;25: 131-43.
- [34] Varma HK, Yokogawa Y, Espinosa FF, Kawamoto Y, Nishizawa K, Nagata F, et al. Porous calcium phosphate coating over phosphorylated chitosan film by a biomimetic method. *Biomaterials* 1999;20:879-84.
- [35] Vallés A. GG, Monleón P. . Biomimetic apatite coating on P(EMA-co-HEA)/SiO<sub>2</sub> hybrid nanocomposites. *Polymer* 2009;50:2874-84.
- [36] Loca D, Narkevica I, Ozolins J. The effect of TiO<sub>2</sub> nanopowder coating on in vitro bioactivity of porous TiO<sub>2</sub> scaffolds. *Materials Letters* 2015;159:309-12.
- [37] Jongwattanapisan P, Charoenphandhu N, Krishnamra N, Thongbunchoo J, Tang IM, Hoonsawat R, et al. In vitro study of the SBF and osteoblast-like cells on hydroxyapatite/chitosan-silica nanocomposite. *Materials Science and Engineering: C* 2011;31:290-9.
- [38] Kujala S, Ryhänen, J., Danilov, A., Tuukkanen, J. Effect of porosity on the osteointegration and bone ingrowth of a weight-bearing nickel-titanium bone graft substitute. *Biomaterials* 2003; 24:4691-7.
- [39] Seo S-J, Kim J-J, Kim J-H, Lee J-Y, Shin US, Lee E-J, et al. Enhanced mechanical properties and bone bioactivity of chitosan/silica membrane by functionalized-carbon nanotube incorporation. *Composites Science and Technology* 2014; 96: 31-7.
- [40] Wu Z, Tang T, Guo H, Tang S, Niu Y, Zhang J, et al. In vitro degradability, bioactivity and cell responses to mesoporous magnesium silicate for the induction of bone regeneration. *Colloids and surfaces B, Biointerfaces* 2014; 120C:38-46.
- [41] Yi W, Sun X, Niu D, Hu X. In vitro bioactivity of 3D Ti-mesh with bioceramic coatings in simulated body fluid. *Journal of Asian Ceramic Societies* 2014.
- [42] Liu CB, R. Preparation of chitosan/cellulose acetate blend hollow fibers for adsorptive performance. *Journal of Membrane Science* 2005; 267: 68-77.
- [43] Martel-Estrada SA, Martínez-Pérez CA, Chacón-Nava JG, García-Casillas PE, Olivas-Armendariz I. Synthesis and thermo-physical properties of chitosan/poly (dl-lactide-co-glycolide) composites prepared by thermally induced phase separation. *Carbohydrate Polymers* 2010; 81: 775-83.
- [44] Aparecida AH, Fook MVL, Santos MLd, Guastaldi AC. Estudo da influência dos íons K<sup>+</sup>, Mg<sup>2+</sup>, SO<sub>4</sub>(2-) e CO<sub>3</sub>(2-) na cristalização biomimética de fosfato de cálcio amorfo (ACP) e conversão a fosfato octacálcico (OCP). *Química Nova* 2007; 30:892-6.
- [45] Lee J, Mahmoud, M., Park, E., Lim, J., Yun, H. A simultaneous process of 3D magnesium phosphate scaffold fabrication and bioactive substance loading for hard tissue regeneration. *Materials science & engineering C* 2014; 36: 252-60.
- [46] Pu X-m, Yao Q-q, Yang Y, Sun Z-z, Zhang Q-q. In vitro degradation of three-dimensional chitosan/apatite composite rods prepared via in situ precipitation. *International journal of biological macromolecules* 2012;51:868-73.
- [47] Aisha MD, Nor-Ashikin MNK, Sharaniza ABR, Nawawi H, Froemming GRA. Orbital fluid shear stress promotes osteoblast metabolism, proliferation and alkaline phosphates activity in vitro. *Experimental Cell Research* 2015;337:87-93.
- [48] Anagnostou F PC, Nefussi JR, Forest N. Role of beta-GP-derived Pi in mineralization via ecto-alkaline phosphatase in cultured fetal calvaria cells. *J Cell Biochem* 1996; 62:262-74.